

The exact numerical solution of a Schrodinger equation with two-Coulomb centres plus oscillator potential

This article has been downloaded from IOPscience. Please scroll down to see the full text article.

1992 J. Phys. A: Math. Gen. 25 3319

(<http://iopscience.iop.org/0305-4470/25/11/034>)

View [the table of contents for this issue](#), or go to the [journal homepage](#) for more

Download details:

IP Address: 171.66.16.58

The article was downloaded on 01/06/2010 at 16:36

Please note that [terms and conditions apply](#).

The exact numerical solution of a Schrödinger equation with two-Coulomb centres plus oscillator potential

D B Khrebtukov†

Eindhoven University of Technology, Department of Physics, P O Box 513, 5600 MB Eindhoven, The Netherlands

Received 13 May 1991, in final form 3 February 1992

Abstract. A numerical technique of solving the Schrödinger equation with two-Coulomb centres plus the oscillator Hamiltonian has been developed. A scheme of evaluating energy levels and wavefunctions of such a Hamiltonian is described in some detail. The proposed algorithm also allows the study of analytical properties of energy levels in a complex plane of the internuclear distance, i.e. to find positions of branch points in the complex plane. The prolate ellipsoidal coordinates enable separation of variables in the equation studied which greatly facilitates the solution. A numerical method for finding branch point positions for an arbitrary analytical function is outlined.

1. Introduction

The main idea of this work was to provide a suitable basis for finding energy levels and wavefunctions of the Hamiltonian proposed by Solov'ev and Vinitzky [1, 2]. When calculating probabilities of various inelastic processes in atomic collisions, use of this Hamiltonian would facilitate taking into account the internuclear axis rotation and electron momentum transfer effects in the most natural way.

The Hamiltonian considered in this work represents an essential part of the Solov'ev–Vinitzky one and consists of two-Coulomb centres and spherical oscillator potentials. The most important feature of this Hamiltonian is the possibility of separating variables in the prolate ellipsoidal coordinates.

Here we describe the method of energy levels and evaluation of wavefunctions using separation of variables, which is similar to that proposed in [3–5]. Further, we discuss the results of energy levels, branch points in the complex plane of internuclear distance and wavefunction calculations.

2. Basic expansions and recurrent equations

We want to find the eigenvalues and eigenfunctions of the following Schrödinger equation (atomic units everywhere unless explicitly stated otherwise):

$$\left\{ -\frac{1}{2}\Delta_r - \frac{Z_1 R}{|r - R/2R|} - \frac{Z_2 R}{|r + R/2R|} + \alpha r^2 \right\} \Psi = E\Psi. \quad (1)$$

† On leave from: A F Ioffe Physical Technical Institute of Academy of Sciences, 194021, Leningrad, Russia.

In prolate ellipsoidal coordinates (defined in appendix A) we can separate variables in equation (1) and obtain three ordinary differential equations connected by separation constants μ and λ :

$$\left\{ \frac{\partial}{\partial \xi} (\xi^2 - 1) \frac{\partial}{\partial \xi} + a\xi - (p_0^2 + \gamma\xi^2) (\xi^2 - 1) - \frac{\mu^2}{(\xi^2 - 1)} - \lambda \right\} X(\xi) = 0$$

$$\left\{ \frac{\partial}{\partial \eta} (1 - \eta^2) \frac{\partial}{\partial \eta} + b\eta - (p_0^2 + \gamma\eta^2) (1 - \eta^2) - \frac{\mu^2}{(1 - \eta^2)} + \lambda \right\} Y(\eta) = 0$$

$$\left\{ \frac{\partial^2}{\partial \varphi^2} + \mu^2 \right\} Z(\varphi) = 0$$

where $p_0 = \sqrt{-E/2}$, $\gamma = \alpha/8$, $a = R(Z_2 + Z_1)$, $b = R(Z_2 - Z_1)$. The boundary conditions require that function $X(\xi)$ should be finite when $\xi \rightarrow 1$ and $\xi \rightarrow \infty$, function $Y(\eta)$ should be finite when $\eta \rightarrow \pm 1$ and $Z(\varphi) = Z(\varphi + 2\pi n)$, $n = 0, 1, 2, \dots$

The equation depending on the azimuth angle can be solved directly, so we have only two non-trivial equations:

$$\left\{ \frac{\partial}{\partial \xi} (\xi^2 - 1) \frac{\partial}{\partial \xi} + a\xi - (p_0^2 + \gamma\xi^2) (\xi^2 - 1) - \frac{m^2}{(\xi^2 - 1)} - \lambda \right\} X(\xi) = 0 \quad (2)$$

$$\left\{ \frac{\partial}{\partial \eta} (1 - \eta^2) \frac{\partial}{\partial \eta} + b\eta - (p_0^2 + \gamma\eta^2) (1 - \eta^2) - \frac{m^2}{(1 - \eta^2)} + \lambda \right\} Y(\eta) = 0 \quad (3)$$

where m is the azimuthal quantum number.

We find the solutions of these two equations by expanding functions $X(\xi)$ and $Y(\eta)$ as follows:

$$X(\xi) = (\xi^2 - 1)^{m/2} \left(\frac{2}{\xi + 1} \right)^\beta \exp \left(-\frac{\sqrt{\gamma}}{2} \xi^2 \right) \sum_{s=0}^{\infty} g_s \left(\frac{\xi - 1}{\xi + 1} \right)^s \quad (4)$$

where $\beta = p_0^2/2\sqrt{\gamma} + m + 1$,

$$Y(\eta) = \exp \left(-\frac{\sqrt{\gamma}}{2} \eta^2 \right) \sum_{l=0}^{\infty} f_l P_{l+m}^m(\eta) \quad (5)$$

where $P_{l+m}^m(\eta)$ are the Legendre functions.

Substituting these expansions in equations (2) and (3) we can write recurrent equations for the expansion coefficients:

$$\kappa_{s+1} g_{s+1} + \kappa_s g_s + \kappa_{s-1} g_{s-1} + \kappa_{s-2} g_{s-2} + \kappa_{s-3} g_{s-3} = 0 \quad (6)$$

$$\delta_{l+2} f_{l+2} + \delta_{l+1} f_{l+1} + \delta_l f_l + \delta_{l-1} f_{l-1} + \delta_{l-2} f_{l-2} = 0 \quad (7)$$

and the coefficients k and δ are

$$\kappa_{s+1} = (s+1)(s+m+1)$$

$$\kappa_s = -4s^2 - 2s(\beta + m + 2\sqrt{\gamma}) + a - \lambda - (\beta - m + 2\sqrt{\gamma})(m + 1)$$

$$\kappa_{s-1} = 6(s - 1)(s + \beta - 1) + 2\lambda + \beta(\beta + m - 4\sqrt{\gamma} + 2) - 2m(m + 1 - 2\sqrt{\gamma})$$

$$\kappa_{s-2} = -4(s - 2)^2 - 2(s - 2)(3\beta - m - 2\sqrt{\gamma}) - a - \lambda - \beta(2\beta - m + 1 - 4\sqrt{\gamma}) - (m + 1)(2\sqrt{\gamma} - m)$$

$$\kappa_{s-3} = (s - 3)(s + 2\beta - m - 3) + \beta(\beta - m)$$

$$\delta_l = (l + m)(l + m + 1) + \sqrt{\gamma}(\beta - m - 1) \left(1 + \frac{4m^2 - 1}{(2(l + m) + 3)(2(l + m) - 1)} \right) - \lambda$$

$$\delta_{l-1} = -b \frac{l}{2(l + m) - 1}$$

$$\delta_{l+1} = -b \frac{l + 2m + 1}{2(l + m) + 3}$$

$$\delta_{l-2} = -2\sqrt{\gamma} \left(l + \beta - \frac{3}{2} \right) \frac{l(l - 1)}{(2(l + m) - 1)(2(l + m) - 3)}$$

$$\delta_{l+2} = 2\sqrt{\gamma} \left(l + 2m - \beta + \frac{5}{2} \right) \frac{(l + 2m + 2)(l + 2m + 1)}{(2(l + m) + 5)(2(l + m) + 3)}$$

The coefficients δ_l reduce to the well known two-Coulomb centres five-member recurrent equation coefficients (e.g. [6]) when $\alpha \rightarrow 0$. In contrast, the coefficients κ_s tend to infinity under the same conditions and this can be explained by the incompatibility of the oscillator's Gaussian asymptotic with that of Coulomb exponential. This incompatibility will be discussed in section 3.3.

3. Results

3.1. Energy levels

Energy levels in the system studied are the eigenvalues of the Hamiltonian in equation (1). To evaluate these one should simultaneously find roots of the two determinants of infinite systems of linear algebraic equations. To be more exact, we should solve the following two equations:

$$\lim_{s \rightarrow \infty} D_s^r(E, \lambda) = 0 \tag{8}$$

$$\lim_{l \rightarrow \infty} D_l^a(E, \lambda) = 0 \tag{9}$$

where $D_s^r(E, \lambda)$ and $D_l^a(E, \lambda)$ are determinants of the first s and l , equations (6) and (7) respectively.

It is easy to see that equation (1) has well known solutions when parameters α and R tend to infinity or to zero.

(i) When $R \rightarrow 0$, equation (1) reduces to a spherical harmonic oscillator problem with equidistant energy levels $E_n = \omega(N + \frac{3}{2})$, where $\omega = \sqrt{2\alpha}$.

(ii) If $\alpha \rightarrow 0$ or $R \rightarrow \infty$ then the energy levels will be very close to those of a two-Coulomb centre (see [5]) multiplied by R^2 .

These properties of equation (1) serve as a very convenient means of checking the proposed algorithm consistency.

The oscillator energy structure is evident in figure 1.

The Coulomb behaviour of energy at large R was used for classification of energy levels. We use parabolic quantum numbers n, n_1, n_2, m of the one-Coulomb centre problem and a symbol of nucleus which this state belongs to at large internuclear separations R : e.g. for $Z_1 = 1$ and $Z_2 = 2$ these nuclei are H and He respectively. It was shown that calculated energy levels can be very well approximated by the usual asymptotic formula for two-Coulomb centres (e.g. [6]) with charges linearly depending on R , i.e. $Z_i \rightarrow Z_i R$.

Finally we can write exact correlation rules to connect parabolic quantum numbers $\{n_1, n_2, m\}$ at large R with elliptic numbers $\{k, q, m\}$ and with spherical numbers of the harmonic oscillator $\{N, l, m\}$ at $R = 0$. Elliptic quantum numbers k and q are equal to the number of zeros of 'radial' and 'angular' wavefunctions respectively, so, noting that the number of zeros should be the same in all three cases, we obtain the following correlation rules:

(i) parabolic to elliptic ($Z_2 > Z_1$):

$$k = n_1 \tag{10}$$

$$q = \begin{cases} \text{for } Z_1\text{-states} & \begin{cases} 2n_2 + n \frac{Z_2 - Z_1}{Z_1} & \text{if } n \frac{Z_2}{Z_1} \text{ is an integer} \\ 2n_2 + 1 + \text{Ent} \left[n \frac{Z_2 - Z_1}{Z_1} \right] & \text{if } n \frac{Z_2}{Z_1} \text{ is not an integer} \end{cases} \\ \text{for } Z_2\text{-states} & \begin{cases} n_2 & \text{if } n_2 < n \frac{Z_2 - Z_1}{Z_2} \\ n_2 + 1 + \text{Ent} \left[n_2 - n \frac{Z_2 - Z_1}{Z_2} \right] & \text{if } n_2 \geq n \frac{Z_2 - Z_1}{Z_2} \end{cases} \end{cases} \tag{11}$$

(ii) elliptic to spherical:

$$N = 2k + q + m \tag{12}$$

$$l = q + m \tag{13}$$

Only equation (12) of the above rules differs from the similar expression for two-Coulomb centres without the oscillator.

We calculated energy levels on the real axis of R in the wide range of the main parabolic quantum number $n = 1, 2, \dots, 5$ and in all cases results were in accordance with these exact correlation rules.

Thus all the facts stated above convince us that our method gives correct values of $E(R)$. The main ideas of the solution algorithm of equations (8) and (9) are outlined in appendix B. We can only state here that the algorithm allows us to calculate energy levels as an analytical function of internuclear distance R in a complex plane of the latter with controllable accuracy of no less than five correct digits.

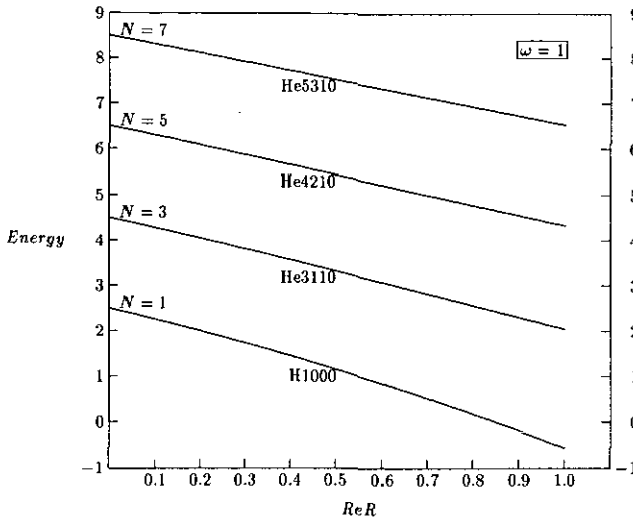


Figure 1. Calculated energy levels for $\alpha = 0.5$ and small R . The harmonic oscillator energy structure is clearly seen at $R = 0$. See discussion of branch points connecting these four levels in subsection 3.2.

3.2. Branch points

It was shown recently that quantitative information on atomic collisions can be obtained when calculating energy levels of a quasimolecular system as an analytical function in a complex plane of internuclear distance R . The positions of branch points of the $E(R)$ function turned out to be connected with regions of inelastic electronic transitions in the quasimolecule. The probability of such a transition can be evaluated using contour integration along a path circumventing a branch point (see [2]).

In contrast to the pure two-Coulomb centres case (see [7]) for fixed charges Z_1 and Z_2 it is not only simple positions of branch points that are relevant but also trajectories of branch points as functions of parameter α play an important role. A method of finding branch points is described in some detail in appendix C.

Some trajectories of branch points are shown in figure 2. Here we have an interesting example of what happens to the analytical structure of the energy levels of two-Coulomb centres in the complex plane of R when dynamic effects represented by α are taken into account†. Figure 2 shows that the higher the energy level, the faster the S -series‡ branch point moves away from the real axis and into the region $\text{Re } R < 0$: in fact the real part of $\text{He4210} \rightarrow \text{He5310}$ branch point turns negative at $\alpha \approx 2$. Because the probability of transition between two energy levels in adiabatic approximation depends on the position of a branch point that connects them, such behaviour of the S -series has serious physical consequences: the most important one consists in a sharp decrease of probability to reach higher energy levels through the S -series.

All the branch points given in figure 2 have a simple square root structure, and the

† For straight line trajectories of nuclear motion $\alpha = \frac{1}{2}(v\rho)^2$, where v is the relative velocity of colliding nuclei and ρ the impact parameter (see [2] for details).

‡ Branch point classification proposed for pure two-Coulomb centres in [7] can also be applied here, because when $\alpha \rightarrow 0$ the positions of branch points tend to those of two-Coulomb centres.

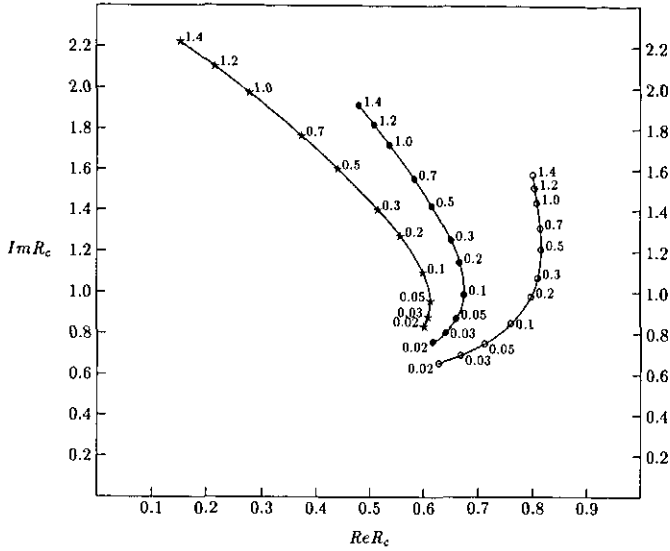


Figure 2 Trajectories of branch points for *S*-series. Numbers beside the points denote the value of α for this point. Symbols: open circle = branch point connecting H1000 energy level with He3110; full circle = the same for He3110 \rightarrow He4210; star = the same for He4210 \rightarrow He5310.

logarithmic behaviour inherent to the *S*-series (see [2]) appears only after combining them. But as the α increases, the distance between these branch points also increases and this leads to the ultimate destruction of logarithmic structure of the Riemann surface here.

3.3. Wavefunctions

The ‘radial’ and ‘angular’ parts of wavefunctions are determined by equations (4) and (5) respectively. The coefficients in these expansions can be found by solving equations (6) and (7) with the zero initial conditions:

$$k_{-1} = k_{-2} = k_{-3} = 0$$

$$\delta_{-1} = \delta_{-2} = 0$$

These systems are self-consistent because the energy and separation constant found in section 3.1 put to zero determinants of these systems of homogeneous algebraic equations. The optimal size of a finite system to be solved can be obtained empirically by checking the convergence of radial and angular parts of wavefunctions as the size is being increased. Usually no more than 20–30 equations are needed for angular wavefunctions, and no more than 50–100 for radial ones.

Radial coefficients g_l and angular coefficients f_l show quite different behaviour as their indices increase. Angular coefficients f_l decrease very rapidly when $l \rightarrow \infty$, and this dependence is not sensitive to the value of parameter α . On the other hand, radial coefficients demonstrate oscillations when $\alpha \rightarrow 0$. After several such oscillations† the radial coefficients also rapidly decrease, so convergence of the sums (4) and (5) is guaranteed in any case.

† The number of oscillations depends on the value of α : the smaller α the more numerous are the oscillations.

Such an oscillatory pattern for the radial coefficients can be explained in the following way. In the radial expansion (4) asymptotics of the corresponding differential equation solution are taken into account explicitly, and the most important part of these is the harmonic oscillator asymptotics $\exp[-(\sqrt{\gamma}/2)\xi^2]$. However, when the oscillator parameter α is very small, there is a certain region of coordinate ξ where the Coulomb part of the Hamiltonian (1) would already behave asymptotically (like $\exp(-p_0\xi)$), although the oscillator is too weak to overshadow an exponential asymptotic with a Gaussian one. So these large oscillations in the values of the radial coefficients serve to 'correct' the difference between these two asymptotics.

After the coefficients of expansions (4) and (5) are found the overall wavefunction should be normalized to represent the amplitude of probability density. Normalizing integrals are

$$\int_{-1}^1 Y^2(\eta) d\eta = 1 \quad (14)$$

$$\int_1^\infty \int_{-1}^1 \frac{1}{8} X^2(\xi) Y^2(\eta) (\xi^2 - \eta^2) d\xi d\eta = 1. \quad (15)$$

It should be noted that we use simple squares of functions $X(\xi)$ and $Y(\eta)$ (in contrast to the usual square of a complex absolute value) in order to preserve analytical properties of the wavefunctions when calculating in the complex plane of R . The normalization in equation (14) is not essential, but it can be performed to reduce the $Y(\eta)$ function to a normalized spherical harmonic when $R \rightarrow 0$.

4. Conclusion

Thus a method of numerical solution of the Schrödinger equation (1) has been developed in this work. The method includes evaluation of equation (1) eigenvalues (energy levels) and eigenfunctions (wavefunctions). Special care was taken to preserve analytical properties of the energy levels and wavefunctions in the complex plane of internuclear distance R , so this method can be used to evaluate positions of branch points which connect different energy levels into one Riemann surface. The knowledge of the branch point positions is very important for calculating probabilities of transitions between different states in atomic collisions.

This work is intended as the first step on the way to solve the Schrödinger equation with the Solov'ev-Vinitsky Hamiltonian (see [2]); this would provide the fullest physical description of binary atomic collisions, including momentum transfer and internuclear axis rotation effects. Energy levels and wavefunctions found in this work will serve as a good initial approximation for the solution of the Solov'ev-Vinitsky modified Schrödinger equation.

Acknowledgments

The author is very grateful to Dr S Y Ovchinnikov for much good and helpful advice which he gave in the course of this work. The author would also like to thank Dr F J de Heer of the FOM Institute (Amsterdam) for his support of this work, and Dr Frans Vitalis (of the same institute) for his great help with computer operation systems.

Appendix A. Prolate ellipsoidal coordinates

Prolate ellipsoidal coordinates can be defined by the following equations:

$$\begin{aligned}\xi &= \frac{r_1 + r_2}{R} & 1 \leq \xi < \infty \\ \eta &= \frac{r_1 - r_2}{R} & -1 \leq \eta \leq 1 \\ \varphi &= \tan^{-1} \left(\frac{y}{x} \right) & 0 \leq \varphi \leq 2\pi\end{aligned}$$

where r_1 and r_2 are the distances from the first and the second centres respectively (see figure 3).

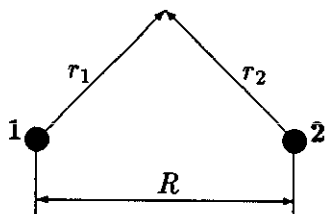


Figure 3. Prolate ellipsoidal coordinates scheme.

The Cartesian coordinates can be expressed in terms of prolate ellipsoidal coordinates in the following way:

$$\begin{aligned}x &= \frac{R}{2} \sqrt{(\xi^2 - 1)(1 - \eta^2)} \cos \varphi \\ y &= \frac{R}{2} \sqrt{(\xi^2 - 1)(1 - \eta^2)} \sin \varphi \\ z &= \frac{R}{2} \xi \eta.\end{aligned}$$

The Laplacian operator in these coordinates is given by

$$\Delta_r = \frac{4}{R^2(\xi^2 - \eta^2)} \left\{ \frac{\partial}{\partial \xi} (\xi^2 - 1) \frac{\partial}{\partial \xi} + \frac{\partial}{\partial \eta} (\eta^2 - 1) \frac{\partial}{\partial \eta} + \frac{\xi^2 - \eta^2}{(\xi^2 - 1)(1 - \eta^2)} \frac{\partial^2}{\partial \varphi^2} \right\}.$$

The differential element of volume is

$$dV = \frac{R^3}{8} (\xi^2 - \eta^2) d\xi d\eta d\varphi.$$

Appendix B. Method of determinant equations solution. Sliding LU decomposition.

To solve the nonlinear equations (8) and (9) we use a quite ordinary gradient method, and the non-trivial part of this solution consists in the way the functions $\lim_{s \rightarrow \infty} D_s^r(E, \lambda)$ and $\lim_{l \rightarrow \infty} D_l^a(E, \lambda)$ are calculated. To evaluate determinants in these functions we use LU decomposition of the relevant matrices. This method is especially effective for matrices with a compact narrow band of non-zero elements along the diagonal, because LU decomposition does not change the band structure and on each step only a limited number of matrix elements is affected. Figure 4 shows the calculation scheme for both radial and angular matrices. The shaded rectangles include matrix elements which take part in LU decomposition on each step. This shaded area slides down the five-diagonal matrix without changing its structure. The determinant is given by the product of the resultant diagonal elements (marked by d letters).

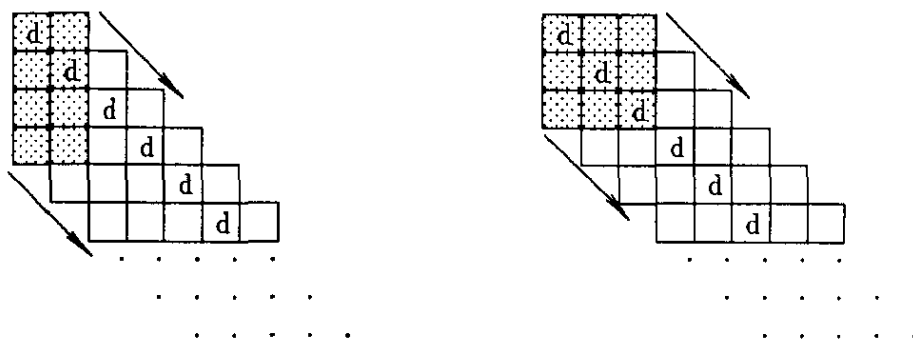


Figure 4. Determinant calculation scheme: radial (left) and angular (right) matrix structures.

Table 1. Empirical values of the coefficient C for different numbers of correct digits in E and λ .

Accuracy \rightarrow	Correct digits		
	≤ 5	6	≥ 7
C	10	12	14

The second important element of the algorithm is the limit calculation in functions $\lim_{s \rightarrow \infty} D_s^r(E, \lambda)$ and $\lim_{l \rightarrow \infty} D_l^a(E, \lambda)$. At large s and l the coefficients in equations (6) and (7) tend to large numbers which depend weakly on E or λ and, therefore, the matrix elements with large numbers only slightly shift the position of a determinant zero. The minimum values of l and s indices when the determinant calculation should stop can be derived from the explicit formulas for coefficients k_s and δ_l .

$$l_{\min} = s_{\min} \geq C \max(\beta, \sqrt{\lambda}).$$

The value of coefficient C depends on the desired number of correct digits in E and λ and the empirical results for the studied variety of energy levels are shown in table 1.

Appendix C. A numerical method of finding root-like branch points

Let us consider an arbitrary function of a complex variable $\mathcal{E}(R)$ and assume that $\mathcal{E}(R)$ has a root-like branch point R_c . This means that in the vicinity of R_c the function behaves approximately like a square root:

$$\mathcal{E}(R) \approx A\sqrt{R - R_c} \quad (16)$$

where A is a constant.

Expression (16) allows us to develop several numerical schemes to find the unknown value of R_c . We used a two-point iterative scheme that was successfully applied by S Y Ovchinnikov (private communication) in the case of the branch points of pure two-Coulomb centres. In this method the value of R_c on the next iteration is given by the following formula:

$$R_{i+1} = R_i + \frac{1}{2} \frac{\mathcal{E}(R_i) - \mathcal{E}(R_{i-1})}{\frac{d\mathcal{E}(R_i)}{dR} - \frac{d\mathcal{E}(R_{i-1})}{dR}} \frac{d\mathcal{E}(R_{i-1})/dR}{d\mathcal{E}(R_i)/dR}. \quad (17)$$

The iterations continue until the condition $|R_{i+1} - R_i| < \varepsilon$ is fulfilled, where ε is the required accuracy of the branch point position. The number of iterations necessary to obtain the required result depends on the initial approximation, and for a good choice of the first point does not exceed 5 or 10. If the initial point is not properly chosen then the iteration step may become too big, but even in this case formula (17) provides the right direction to the branch point, so the latter can still be found by reasonably limiting the iteration step in this direction.

References

- [1] Solov'ev E A and Vinitsky S I 1985 *J. Phys. B: At. Mol. Phys.* **18** L557-62
- [2] Solov'ev E A 1989 *Sov. Phys. Usp.* **32** 228
- [3] Jaffe G 1934 *Z. Phys.* **87** 535
- [4] Baber W G and Hassé H R 1935 *Proc. Camb. Phil. Soc.* **31** 564
- [5] Bates D R and Carson T R 1956 *Proc. R. Soc. A* **234** 207
- [6] Komarov I V, Ponomarev L I and Slavianov S Yu 1976 *Spheroidal and Coulomb Spheroidal Functions* (Moscow: Nauka)
- [7] Ovchinnikov S Y and Solov'ev E A 1986 *Sov. Phys.-JETP* **63** 538